AIP | Journal of Applied Physics

Barrier height and tunneling aspects in (110) CrO2 with its natural barrier

M. Pathak, D. Mazumdar, V. Karthik, X. Zhang, K. B. Chetry, S. Keshavarz, P. LeClair, and A. Gupta

Citation: Journal of Applied Physics **110**, 053708 (2011); doi: 10.1063/1.3626471
View online: http://dx.doi.org/10.1063/1.3626471
View Table of Contents: http://scitation.aip.org/content/aip/journal/jap/110/5?ver=pdfcov
Published by the AIP Publishing

Articles you may be interested in

Magnetic and magnetotransport properties of half-metallic CrO2-SnO2 composites
J. Appl. Phys. **114**, 233903 (2013); 10.1063/1.4844595

Low temperature tunneling magnetoresistance on (La , Sr) Mn O 3／Co junctions with organic spacer layers
J. Appl. Phys. **103**, 093720 (2008); 10.1063/1.2924435

Magnetostriction and tunneling magnetoresistance of Co Fe B／Al O x／Co／Ir Mn junctions
J. Appl. Phys. **103**, 07A901 (2008); 10.1063/1.2828543

Magnetic tunnel junctions based on Cr O 2／Sn O 2 epitaxial bilayers
Appl. Phys. Lett. **89**, 022511 (2006); 10.1063/1.2216109

Spin-polarized transport in hybrid (Zn , Cr) Te／Al 2 O 3／Co magnetic tunnel junctions
Appl. Phys. Lett. **88**, 202501 (2006); 10.1063/1.2205177

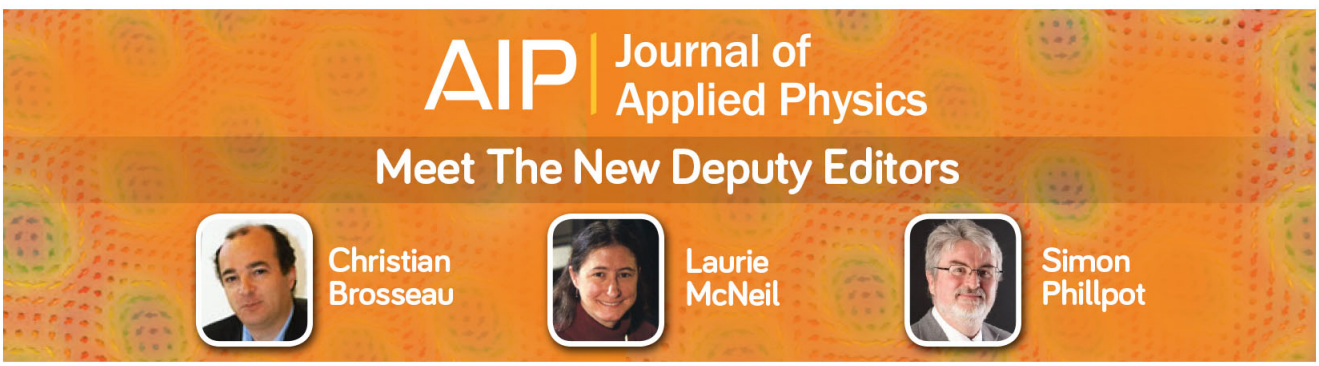

[This article is copyrighted as indicated in the article. Reuse of AIP content is subject to the terms at: http://scitation.aip.org/termsconditions. Downloaded to] IP: 131.230.106.30 On: Wed, 21 Jan 2015 18:19:01

Barrier height and tunneling aspects in (110) CrO_2 with its natural barrier

M. Pathak,[1,2] D. Mazumdar,[2] V. Karthik,[2] X. Zhang,[2,3] K. B. Chetry,[1,2] S. Keshavarz,[1,2] P. LeClair,[1,2] and A. Gupta[2,3,a)]
[1]*Department of Physics and Astronomy, University of Alabama, Tuscaloosa, Alabama 35487, USA*
[2]*MINT Center, University of Alabama, Tuscaloosa, Alabama 35487, USA*
[3]*Department of Chemistry, University of Alabama, Tuscaloosa, Alabama 35487, USA*

(Received 14 February 2011; accepted 20 July 2011; published online 9 September 2011)

We have investigated (110) CrO_2/natural barrier/Co magnetic tunnel junctions for their barrier and magneto-transport properties. A negative tunnel magnetoresistance (TMR) of over 5% was observed in micro-fabricated devices at 4.2 K, which is comparable to TMR values obtained with (100) CrO_2. Both transport and cross-sectional transmission electron microscopy analysis reveal a natural barrier thickness 3.5 ± 0.5 nm. However, we obtain a low effective barrier height of 0.4 eV from transport measurements. The inelastic electron tunneling spectroscopy showed significant bias dependence with peak positions showing vibrational modes, which deviate from stoichiometric Cr_2O_3. We conclude that the transport characteristics are controlled by defects within the natural barrier, consistent with recent theoretical reports. © *2011 American Institute of Physics*. [doi:10.1063/1.3626471]

I. INTRODUCTION

Because of the experimentally observed high spin polarization in CrO_2 thin films;[1,2] magnetic tunnel junctions with CrO_2 as an electrode have been the focus of intense research for both its fundamental and technological implications.[3,4] So far, tunnel magnetoresistance (TMR) value consistent with its high spin-polarization has not been reported in a device with CrO_2 as an electrode.[3,4] Observed TMR in CrO_2/natural barrier/Co junctions at 4.2 K has been $\sim 8\%$;[3] with Leo *et al*. showing that the sign of TMR changes from negative to positive with the insertion of a thin Mg layer probably by preventing the growth of the natural barrier.[4] The thin, natural, stable and insulating oxide of Cr on top of CrO_2 thin films that is used as the tunneling barrier in these junctions has been attributed to be the most stable oxide of Cr, i.e., Cr_2O_3 or an oxygen-deficient variant (CrO_x, $x < 1.5$). In this work we probe the transport characteristics through the natural barrier, grown on (110)-oriented CrO_2 junction. I-V characteristics estimate the barrier height in the CrO_2/natural barrier/Co junction and provide information about the barrier itself and valuable physical insight into the transport mechanism. Also, all the previously reported CrO_2 devices are on epitaxial (100) CrO_2 films grown on isostructural TiO_2 substrates. As has been recently found by our group, epitaxial (100) CrO_2 films are subject to substrate-induced strain up to significantly high film thickness ($\sim$200 nm) while (110) CrO_2 films grow strain-free when grown on respective TiO_2 substrates[5,6]—with (100) CrO_2 films following layer-by-layer growth while (110) CrO_2 films showing island-like growth modes. The room temperature magnetization value of (110) CrO_2 is also substantially enhanced compared to (100) CrO_2 due to strain-free growth. Therefore, if exploited properly, it is expected to translate to better CrO_2 device performance. With this motivation, we investigated devices with (110) CrO_2 as the high spin-polarization electrode.

II. EXPERIMENT

For our experiment, we deposited the CrO_2 layer on (110) TiO_2 substrate using the selective growth method described previously.[7] The (110) CrO_2 film thickness in case of all the results reported here is 50 nm. To get the robust natural insulating barrier, the CrO_2 film is kept under ambient conditions for about two weeks. The film is then patterned using standard photolithography technique to define the TMR devices for our experiment. Co ($\sim$60 nm) and Au ($\sim$30 nm) were sputtered in a vacuum chamber with base pressure less than 5×10^{-7} Torr to grow the free magnetic layer and the capping layer, respectively, in TMR devices. We observed that the devices are shorted and did not show any TMR if they are fabricated immediately after selectively growing the (110) CrO_2 film. This indicates that the natural barrier evolves with time. The cross-sectional images were obtained in a FEI Tecnai F20 transmission electron microscope (TEM). Fabricated devices were tested for their TMR properties in a home-made measurement set-up at liquid nitrogen temperature ($\sim$78 K) since the devices did not show any room temperature TMR—as reported previously.[3,4] Distinct magnetic switching is important to observe TMR effect, which in our case is 100 Oe and 400 Oe for the Co and CrO_2 layers, respectively, at 78 K. No significant effect of shape anisotropy was observed on the switching and TMR behavior and the reported result here is for a typical junction of size $3 \times 6\ \mu m^2$. Temperature-dependent TMR data and I-V properties were obtained in a Quantum Design physical property measurement system (PPMS). Inelastic electron tunneling spectroscopy (IETS) on the device(s) was collected with our home-made measurement set-up and attaining the low temperature of 2 K for this measurement in the PPMS. Details of our IETS measurement are described later with the results.

a)Electronic mail: agupta@mint.ua.edu.

 © 2011 American Institute of Physics

[This article is copyrighted as indicated in the article. Reuse of AIP content is subject to the terms at: http://scitation.aip.org/termsconditions. Downloaded to] IP: 131.230.106.30 On: Wed, 21 Jan 2015 18:19:01

All reported I-V and IETS spectra here are averaged from several repeated scans between ±100 mV.

III. RESULTS AND DISCUSSION

We first present our TEM analysis which provides information about the barrier thickness and film microstructure in an unambiguous manner. Figure 1(a) shows the bright-field TEM images of CrO_2/natural barrier/Co tunnel junction deposited on (110) TiO_2 substrates taken along the (110) zone-axis. As shown in this figure, the insulating barrier (the bright contrast between Co and CrO_2) was found to have relatively sharp interfaces with a thickness of about 3.5 ± 0.5 nm (agrees well with the Brinkman, Dynes, and Rowell (BDR) fit for barrier thickness, as discussed later). The variation in barrier thickness (0.5–1.0 nm) is consistent with inherent roughness of (110) CrO_2 films.[5] The high resolution TEM image in Fig. 1(b) shows the homo-epitaxial growth of (110) CrO_2 with lattice fringes corresponding to the orientation relationship (110) CrO_2||(110) TiO_2 and also polycrystalline growth of the Co layer on top of the natural barrier. The TiO_2/CrO_2 interface shows the presence of misfit dislocations. Note that the CrO_2/natural barrier interface shows little contrast owing to the strain-free growth of natural barrier. As seen in the figure, the natural barrier exhibits a crystalline structure close to CrO_{2-x} as reported previously.[4] However, the natural barrier/Co interface exhibits a dark contrast owing to stacking fault-like defects, which could also be a major source of spin-scattering.

As shown in Fig. 2, the junction resistance of the device increases from 300 K to 2 K when measured in PPMS with four point probe method and dc current of 1.0 μA. Junction resistance is close to 2 kΩ from 300 K to ~200 K, and it increases almost 3 times (~5.5 kΩ) at 2 K. This indicates that tunneling is the most likely mode of transport in this device. An increase in junction resistance can be attributed to a few factors. Both metallic electrodes' (CrO_2 and Co) resistance decreases significantly with decreasing temperature (not shown). Also, thermal fluctuations are reduced with decreasing temperature. Increasing magnetic moment with decreasing temperature[6] also contributes to the increase in the resistance of the junction via spin-dependent tunneling.[8] TMR observed in this device is −5.3% at 4 K (Fig. 3), which is similar to negative TMR observed in devices with (100) CrO_2.[3,4] Also, no noticeable TMR was observed at temperatures above 200 K (data not shown), which is also similar to (100) CrO_2 device performances.

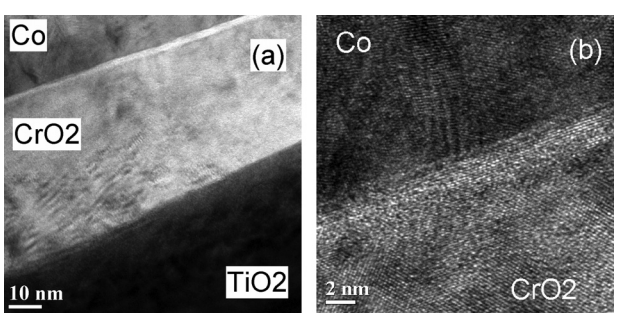

FIG. 1. TEM micrograph of CrO_2/natural barrier/Co layers on (110) TiO_2 substrate. (a) shows the sharp interface with the natural barrier and (b) is the high resolution image around the natural barrier.

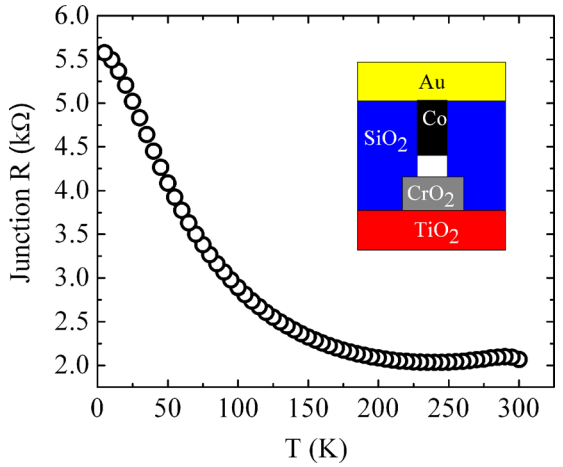

FIG. 2. (Color online) Typical resistance against temperature behavior of a CrO_2/natural barrier/Co device. Lateral schematic diagram of the device is shown in the inset. SiO_2 was deposited to keep the top and bottom electrodes electrically isolated. The region between Co and CrO_2 is the natural insulation barrier.

Assuming spin polarization of CrO_2 to be 98% and that of Co to be −42%, then according to the Julliere model,[9] TMR value for this junction is expected to be about −57% at low temperature. The observed TMR is much lower than the expected value. This indicates that there is significant spin-flip process(es) taking place at the interface(s) with the barrier. As CrO_x—the presumed tunneling barrier in our devices is known to be weakly antiferromagnetic;[10] significant spin-flip scattering at the barrier interfaces is likely to reduce the TMR effect. Also, (110) CrO_2 follows island-like growth mode on isostructural TiO_2 substrates and roughness values of about 1.0 nm for a 50 nm film[5] might possibly make the barrier less effective to observe a significant TMR effect, e.g., by promoting ferromagnetic (FM) coupling of the electrodes or intermixing. The sign of TMR in a CrO_2-based device is also very

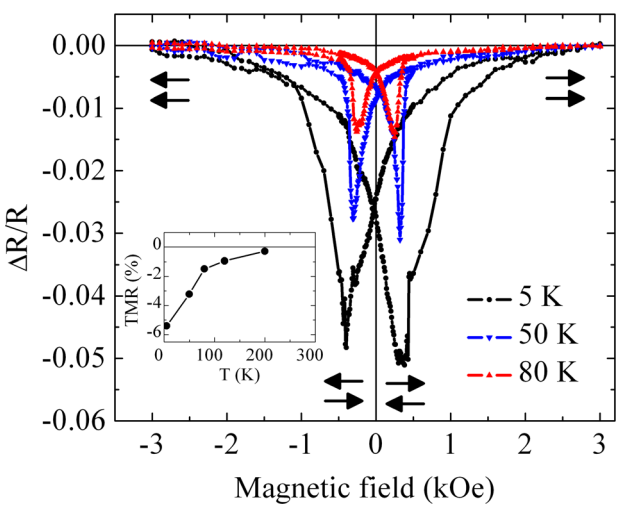

FIG. 3. (Color online) TMR of the device at three different temperatures. Temperature dependence of TMR is shown in the inset. The arrows represent the relative orientations of the top and bottom magnetic layers with applied magnetic field.

[This article is copyrighted as indicated in the article. Reuse of AIP content is subject to the terms at: http://scitation.aip.org/termsconditions. Downloaded to] IP: 131.230.106.30 On: Wed, 21 Jan 2015 18:19:01

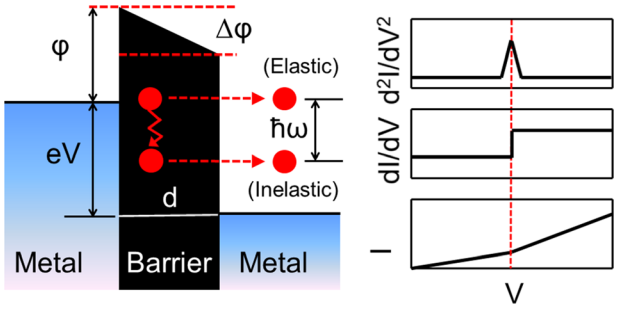

FIG. 4. (Color online) Schematic energy diagram of IETS phenomenon between two metal electrodes sandwiching an insulating barrier. The increase in current due to inelastic tunneling of electrons at a particular voltage and corresponding changes in its first and second derivative are schematically shown.

interface sensitive.[6] However; in our devices, observed negative TMR is attributed to the negative spin polarization of top Co layer while the CrO_2 layer maintains a positive spin polarization due to conduction of only majority electrons.[3] We next focus on the tunnel barrier properties.

Like in other tunnel junctions, the barrier in CrO_2/natural barrier/Co junction can be studied by observing its I-V characteristics (as shown in the schematic energy diagram Fig. 4). Barrier height (φ) is the potential barrier provided by the insulator of thickness d between the ferromagnetic electrodes. Asymmetry in the barrier arises because of the different work functions involved with CrO_2 and Co. Based on the I-V characteristics of our tunneling devices; we used two models to estimate the barrier height in the junctions. The Brinkman, Dynes, and Rowell (BDR) model[11–13] assumes a trapezoidal barrier as shown in Fig. 4. According to this model, conductance of the junction is expressed as a polynomial function of bias voltage up to 2nd order,

$$\frac{dI}{dV} = A + BV + CV^2 \tag{1}$$

and, thus giving current in the device against bias voltage:

$$I = AV + \frac{BV^2}{2} + \frac{CV^3}{3}, \tag{2}$$

where A, B, and C are constants evaluated by fitting experimental data with, $I(V=0)=0$. On getting the constants A, B, and C from fitting barrier thickness (in angstroms), barrier height (in electron volts) and barrier asymmetry (in electron volts) can be calculated from the BDR model according to the following expressions:

$$d^2 = -5.368\sqrt{\frac{C}{A}}\ln\left(1.747\times10^{-10}\sqrt{\frac{C}{A}}\right), \tag{3}$$

$$\varphi = 0.03281\left(\frac{A}{C}\right)d^2, \tag{4}$$

$$\Delta\varphi = -23.42\left(\frac{B}{A}\right)\frac{\varphi^{3/2}}{d}. \tag{5}$$

Both current and conductance in the device are fitted with the BRD model as shown in Figs. 5(a) and 5(b), respectively. We

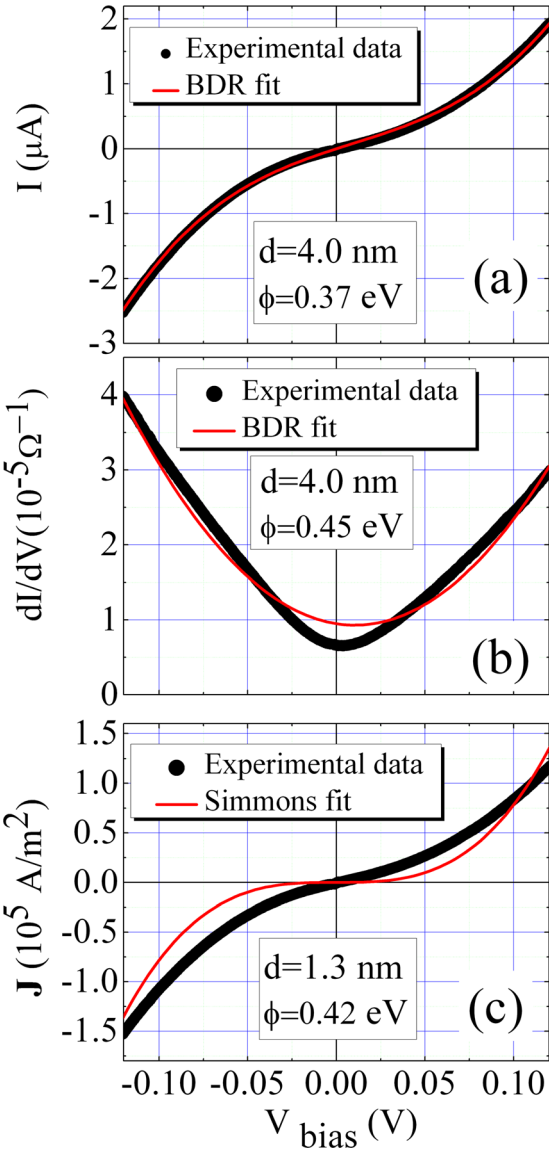

FIG. 5. (Color online) Fitting of current (a) and conductance (b) against bias voltage with BDR model. (c) Current density against bias voltage in the device with Simmons fit.

extract a barrier thickness of 4.0 nm, using both current and conductance fitting, which is in good agreement with direct barrier thickness estimation in TEM, i.e., 3.5 ± 0.5 nm. Also, this barrier thickness is close to three times the lattice parameter c in Cr_2O_3 ($a = 0.496$ nm, $c = 1.36$ nm for its hexagonal corundum structure,[14] assuming, of course, that structural lattice parameter of the barrier is close to Cr_2O_3.

Further, we also fitted the current density curves using the Simmons model,[15] as comparison between the barrier heights is still relevant as it is not *a priori* clear, beyond the reasons mentioned above, which model best describes transport properties. The model proposed by Simmons[15] assumes a rectangular shaped ideal barrier between two metallic electrodes. According to his model, current density across the junction for intermediate voltages can be approximated by

$$J = \beta(V + \gamma V^3), \tag{6}$$

[This article is copyrighted as indicated in the article. Reuse of AIP content is subject to the terms at: http://scitation.aip.org/termsconditions. Downloaded to] IP: 131.230.106.30 On: Wed, 21 Jan 2015 18:19:01

where,

$$\beta = \frac{3}{2d}\left(\frac{e}{\hbar}\right)^2 (2m\varphi)^{1/2} \exp\left[-\left(\frac{4\pi d}{\hbar}\right)(2m\varphi)^{1/2}\right] \quad (7)$$

and

$$\gamma = \frac{\pi m}{3\varphi(ed/\hbar)^2}. \quad (8)$$

Here, φ is the potential barrier height in electron volts, d is the barrier thickness in nanometers, m is the mass of electron, and $\hbar$ is reduced Plank's constant. For low bias, Eq. (6) can further be approximated to $J = \beta V$, neglecting the cubic potential term. There are significant differences between the BDR model and the Simmons model in that the barrier asymmetry is not captured in the Simmons formula. This can be understood by noting that the Simmons model lacks the quadratic term, which captures asymmetry in the BDR formula. Therefore, not surprisingly as seen in Fig. 5(c), the Simmons model does not give a very good fit of the current densities against applied bias voltages. Estimates of barrier height provided a value of 0.42 eV at 78 K with barrier thickness 1.3 nm, and 0.10 eV for barrier thickness of 3.5 nm.

Both current and conductance fittings in the BDR model gave higher barrier asymmetry than barrier height. It is possible that none of the barrier models (BDR or Simmons) provides a good description, and a more elaborate multiple barrier fitting is more suitable for this junction, as it enters the regime of Fowler-Nordheim tunneling.[16] However such considerations are beyond the scope of this present work and, therefore, we instead focus on understanding the barrier properties. Considering effective barrier height to be $\varphi + \Delta\varphi/2$, from current fit it is 0.37 eV and from conductance fit it is 0.45 eV according to BDR model. This barrier height is smaller than the barrier height of 0.76 eV reported by Barry *et al.* in a similar junction with (100) CrO_2.[17] All these barrier heights are much smaller than the energy gap of 3.0 eV between the conduction band and the valance band of Cr_2O_3 observed by Cheng *et al.* in XPS study of naturally grown Cr_2O_3 on CrO_2 metallic surface.[18]

The low barrier height value is intriguing. In Ref. 12, Miller and Belyea have argued that observation of intrinsically large barrier heights is unlikely in transport measurements as presence of defects, even at very low defect levels. This scenario is very likely at play here. In a later analysis we show that chemically the barrier deviates significantly from stoichiometric Cr_2O_3, which provides us evidence that defects within the tunnel barrier could govern transport and not the electrode material properties (roughness for instance) or its orientation. Such defects could be related to oxygen vacancies within the barrier, which introduces defect states in the bandgap of the insulator, lowering the barrier height of transport. The only other possibility that could lead to low effective barrier height are intrinsic band structure effects, as observed in the case of band-matched Fe/MgO.[19] In this case, highly dispersive conduction and valence bands give rise to a low electronic effective mass, and therefore a low height. But such band-matching is unlikely due to lattice-symmetry mismatch between cubic CrO_2 and hexagonal Cr_2O_3.

The chemical nature of the natural barrier is probed by the IETS technique. Compared to the total current through the junction, the increase in current due to IETS (shown schematically in Fig. 4) is very small—within 1% of the total current and therefore may not be more significant than the electrical noise level at room temperature. The full width at half maxima (FWHM) of the IETS peak has a temperature dependence of $5.4k_BT$ (Ref. 20) and therefore to obtain a significant resolution, spectra were taken at 2 K, which corresponds to a thermal broadening of 0.93 mV. Because of asymmetry in barrier energy, inelastic tunneling electrons also see different barrier height depending on the bias polarity and accordingly their peak intensities can depend on the bias voltage polarity of the device.[21] The IETS signal is obtained, considering a small ac modulation ($V_m \cos \omega t$) with the dc bias (V_b) across the junction as the 2nd order term in the following expansion:

$$I(V_b + V_m \cos \omega t) = I(V_b) + \left.\frac{dI}{dV}\right|_{V_b} V_m \cos \omega t + \left.\frac{d^2I}{dV^2}\right|_{V_b} V_m^2 \cos^2 \omega t + \cdots. \quad (9)$$

For a bias voltage of 150 mV, modulation voltage was 1–2 mV with modulation frequency ~1 kHz to get rid of any low frequency noise. Calculated minimum energy resolution due to ac modulation is 1.22 V_m (Ref. 20) and therefore for an ac modulation of 2.0 mV, IETS spectra can be confirmed to be correct within ±2.5 mV. Modulation broadening of the IETS spectra is therefore on the same order as thermal broadening at 2 K, which is about 1.0 mV.

Figure 6 shows the IETS spectra obtained on one of our devices at 2 K for positive and negative biases. Observed intensities in the spectra were smaller for positive bias between CrO_2 and Co than negative bias and correspondingly peak intensities are also smaller for positive bias.

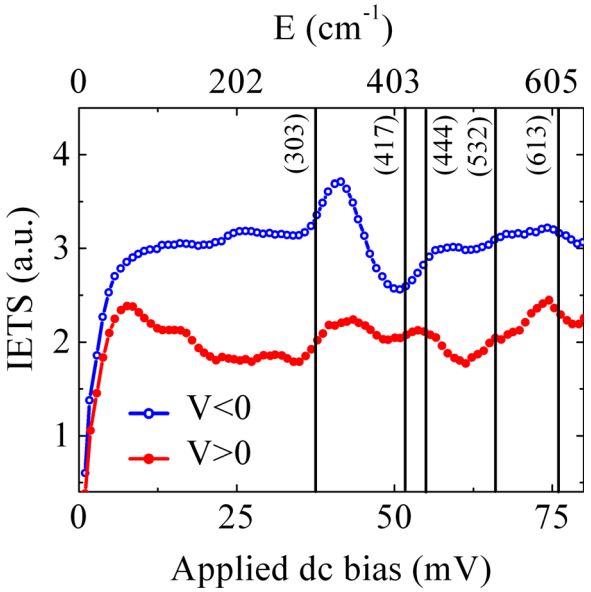

FIG. 6. (Color online) IETS spectra obtained in the (110) CrO_2/natural barrier/Co junction for positive and negative biases. Vertical lines show the positions of a few Cr_2O_3 vibrational lines from infrared spectroscopy.

[This article is copyrighted as indicated in the article. Reuse of AIP content is subject to the terms at: http://scitation.aip.org/termsconditions. Downloaded to] IP: 131.230.106.30 On: Wed, 21 Jan 2015 18:19:01

Energies of the vibrational modes in bulk Cr_2O_3 obtained with infrared spectroscopy are shown in Fig. 6 by the vertical lines.[22] From left to right, the positions of these lines are 303, 419, 444, 532, and 613 cm^{-1}, respectively. Considering the peak positions to be correct within ± 2.5 mV and comparing with the available data, these peak positions can be assigned to off-stoichiometric Cr_2O_3 excitations. Also, because of the strong bias and temperature dependence of our IETS spectra, it was not corrected for the elastic tunneling background.[21] As discussed in our transport analysis, we conclude in general that precise characterization of the natural barrier, apart from the electrode material, in CrO_2 devices can play a decisive role in determining the magneto-transport properties of tunnel junctions.

IV. SUMMARY

In summary, micro-fabricated (110) CrO_2/natural barrier/Co tunnel junctions were investigated for their TMR, I-V characteristics, and inelastic tunneling spectroscopy (IETS). The TMR response and its temperature dependence are similar to previously reported results with (100) CrO_2 as an electrode. The barrier height obtained from the I-V characteristics of the junction is approximately 0.40 eV, which is lower than anticipated values. However, the estimated barrier thickness from I-V characteristics matches reasonably well with the thickness of the natural oxide layer on CrO_2 film observed in TEM. The IETS spectra had significant bias dependence and the IETS peak positions showed vibrational modes to deviate from stoichiometric Cr_2O_3. Based on the overall transport characteristics, we conclude that tunneling properties to be determined by defects within the barrier material and not by the high spin-polarized CrO_2 or its crystallographic orientation.

ACKNOWLEDGMENTS

We thank UA MFF, especially Dr. Alton Highsmith for helping with the device fabrication. This work was supported by NSF under Grant No. DMR-0706280.

[1]J. Parker, S. Watts, P. Ivanov, and P. Xiong, Phys. Rev. Lett. **88**, 196601 (2002).
[2]A. Anguelouch, A. Gupta, G. Xiao, D. W. Abraham, Y. Ji, S. Ingvarsson, and C. L. Chein, Phys. Rev. B **64**, R180408 (2001).
[3]A. Gupta, X. W. Li, and G. Xiao, Appl. Phys. Lett. **78**, 1894 (2001).
[4]T. Leo, C. Kaiser, H. Yang, S. S. P. Parkin, M. Sperlich, G. Güntherordt, and D. J. Smith, Appl. Phys. Lett. **91**, 252506 (2007).
[5]K. B. Chetry, M. Pathak, P. LeClair, and A. Gupta, J. Appl. Phys. **105**, 083925 (2009).
[6]M. Pathak, H. Sato, X. Zhang, K. B. Chetry, D. Mazumdar, P. R. LeClair, and A. Gupta, J. Appl. Phys. **108**, 053713 (2010).
[7]A. Gupta, X. W. Li, S. Guha, and G. Xiao, Appl. Phys. Lett. **75**, 2996 (1999).
[8]P. M. Tedrow and R. Meservey, Phys. Rev. Lett. **26**, 192 (1971).
[9]M. Julliere, Phys. Lett. **54A**, 225 (1975).
[10]T. R. McGuire, E. J. Scott, and F. H. Grannis, Phys. Rev. **102**, 1000 (1956).
[11]W. F. Brinkman, R. C. Dynes, and J. M. Rowell, J. Appl. Phys. **41**, 1915 (1970).
[12]C. W. Miller and D. D. Belyea, J. Appl. Phys. **105**, 094509 (2009).
[13]C. W. Miller and D. D. Belyea, Appl. Phys. Lett. **96**, 022511 (2010).
[14]G. K. Lewis, Jr. and H. G. Drickamer, J. Chem. Phys. **45**, 224 (1966).
[15]J. G. Simmons and G. J. Unterkofler, J. Appl. Phys. **34**, 1828 (1963).
[16]C. W. Miller, Z.-P. Li, I. K. Schuller, R. W. Dave, J. M. Slaughter, and J. Akerman, Phys. Rev. B **74**, 212404 (2006).
[17]A. Barry, J. M. D. Coey, and M. Viret, J. Phys.: Condens. Matter **12**, L173 (2000).
[18]R. Cheng, B. Xu, C. N. Borca, A. Sokolov, C. S. Yang, L. Yuan, S. H. Liou, B. Doudin, and P. A. Dowben, Appl. Phys. Lett. **79**, 3122 (2001).
[19]W. H. Butler, X. G. Zhang, T. C. Schultess, and J. M. MacLaren, Phys. Rev. B **63**, 54416 (2001).
[20]P. K. Hansma, *Tunneling spectroscopy: Capabilities, Applications, and New Techniques* (Plenum, New York, 1982).
[21]J. W. Reiner, S. Cui, Z. Liu, M. Wang, C. H. Ahn, and T. P. Ma, Adv. Mater. **XX**, 1 (2010).
[22]D. R. Renneke and D. W. Lynch, Phys. Rev. **138**, A530 (1965).

[This article is copyrighted as indicated in the article. Reuse of AIP content is subject to the terms at: http://scitation.aip.org/termsconditions. Downloaded to] IP: 131.230.106.30 On: Wed, 21 Jan 2015 18:19:01